Saudi Journal of Biological Sciences (2015) xxx, xxx–xxx

King Saud University

Saudi Journal of Biological Sciences

www.ksu.edu.sa
www.sciencedirect.com

ORIGINAL ARTICLE

# Enhancing antidiabetic and antimicrobial performance of *Ocimum basilicum*, and *Ocimum sanctum* (L.) using silver nanoparticles

**Veshara Malapermal [a], Izel Botha [b], Suresh Babu Naidu Krishna [a], Joyce Nonhlanhla Mbatha [a,*]**

[a] *Department of Biomedical and Clinical Technology, Faculty of Health Science, Durban University of Technology, Durban, South Africa*
[b] *Department of Homeopathy, Durban University of Technology, Durban, South Africa*

Received 23 April 2015; revised 24 June 2015; accepted 28 June 2015

**KEYWORDS**

*Ocimum basilicum*;
*Ocimum sanctum*;
Silver nanoparticles;
AgNps;
α-Glucosidase;
Diabetes mellitus

**Abstract** The role of silver nanoparticles (AgNps) is an attractive proposition for advancing modern diabetes therapies and applied science. Stable AgNps with a size range of 3–25 nm were synthesized using aqueous leaf extracts from *Ocimum basilicum*, *Ocimum sanctum*, and in combination. The concentration of the extracts facilitated the reduction of silver nitrate that led to the rapid formation of AgNps at room temperature, indicating a higher reaction rate as opposed to harsh chemical methods, and high conversion energy usually involved in the synthesis. The size, shape and elemental analysis were carried out using UV–Visible spectroscopy, transmission electron microscopy (TEM), scanning electron microscopy with energy-dispersive X-ray spectroscopy (SEM–EDX), dynamic light scattering (DLS), and zeta potential whilst, Fourier transform infrared (FTIR) supported by gas chromatography mass spectroscopy (GC–MS) was used to identify the type of capping agents. Inhibition of α-amylase and α-glucosidase enzymes retards the rate of carbohydrate digestion, thereby provides an alternative and a less evasive strategy of reducing postprandial hyperglycaemia in diabetic patients. The AgNps derived from *O. sanctum* and *O. basilicum*, respectively displayed an inhibitory effect at 89.31 ± 5.32%, and 79.74 ± 9.51%, respectively, against *Bacillus stearothermophilus* α-glucosidase enzyme model, indicating an enhanced biocatalytic potential compared to their respective crude extracts and the control. Furthermore, the emerging rate of infections in diabetic patients validates the need for the discovery of dual diabetes therapies. As a result, the bioderived AgNps displayed antimicrobial activity against bacterial

* Corresponding author. Tel.: +27 31 3735280; fax: +27 31 3735295.
E-mail address: nonhlanhlam@dut.ac.za (J.N. Mbatha).
Peer review under responsibility of King Saud University.

Production and hosting by Elsevier

http://dx.doi.org/10.1016/j.sjbs.2015.06.026


Please cite this article in press as: Malapermal, V. et al., Enhancing antidiabetic and antimicrobial performance of *Ocimum basilicum*, and *Ocimum sanctum* (L.) using silver nanoparticles. Saudi Journal of Biological Sciences (2015), http://dx.doi.org/10.1016/j.sjbs.2015.06.026

species *Staphylococcus aureus*, *Escherichia coli*, *Pseudomonas aeruginosa*, *Bacillus subtilis*, and *Salmonella* species.



## 1. Introduction

The new era in diabetes treatment facilitates the rapid green synthesis of multifunctional, biocompatible, and eco-friendly metal colloidal nanoparticles (Nps), as effective nanomedicine against the emerging threat of diabetes mellitus (DM), and as a result the harsh environmental impact of its associated complications (Alkaladi et al., 2014; Karthick et al., 2014). Worldwide, DM is estimated to reach 592 million people by the year 2035, with a prevalence of 8.3% (Guariguata et al., 2014). The increased prevalence is owing to five main influences, modernization of lifestyle, obesity, aged population, ethnicity, and unavoidable genetic predisposition (Hannan et al., 2006). By convention, DM is classified into two main types, Type I DM (IDDM, insulin dependent diabetes mellitus), treated with insulin replacement therapy, whilst diet, lifestyle modifications and oral antidiabetic drugs are considered the foundation for the treatment and management of Type II DM (NIDDM, non-insulin dependent diabetes mellitus). Despite the popularity of insulin and oral antihyperglycaemic drugs, epidemiological studies and clinical trials strongly support the notion that the prolonged use of such agents fail to prevent the progression of long-term complications such as, diabetic retinopathy, neuropathy, nephropathy, foot infections, atherosclerosis and other associated cardiovascular events, including hypertension, obesity, dyslipidemia, and hypercoagulability (Avery et al., 2008; Ratner, 2001). The main drawback of insulin is that they are associated with fear of painful injections, poor patient compliance, complex to use and prescribe, potential dosing errors, diabetic ketoacidosis, local tissue necrosis, infection, nerve damage, whilst cost and iatrogenic hypoglycaemia will continue to be an important limiting factor (Mo et al., 2014; Cryer, 2008). Research indicates that most oral antihyperglycaemic agents cannot maintain normal levels of blood glucose for an extended period of time, especially in the elderly (Avery et al., 2008) and gestational diabetes during pregnancy (Swarnalatha et al., 2012). These agents also pose risks of hypoglycaemia, cardiovascular diseases, weight gain, gastrointestinal (GI) disturbances (severe lactic acidosis), liver injury, renal complications, and hypersensitivity reactions (Reid et al., 2012), therefore, making the development of effective antidiabetic agents as one of the world's top public health priorities.

Applications of engineered Ag, Au, Fe, Pt, Zn, etc. and metal oxide Nps have evolved positively, influencing medicine, science, and many new agro-food industries (Bouwmeester et al., 2009). Nps offer unique self-assembly properties, size dependent crystalline structure (1–100 nm), greater surface to volume ratios, stability, specificity, drug encapsulation, surface structure and biocompatibility due to their material composition (Venkatachalam et al., 2013; Ehdaie, 2007). Thus, nanomedicine facilitates the production and application of devices or materials to interact with the human body at a molecular level with a high degree of specificity, this can potentially be translated into targeted cellular and tissue-specific clinical applications, designed to achieve maximal therapeutic efficacy with minimal to no side effects (Sahoo et al., 2007). The success rate of nanomedicine can be observed in its attempts for treatment of lung cancer (Gengan et al., 2013), acute myeloid leukaemia (AML) (Guo et al., 2013), colon cancer (Prabhu et al., 2013), HIV-1 (Gavanji et al., 2014), plasmodial (Panneerselvam et al., 2015), fungal, and bacterial infections (Lokina et al., 2014).

The metal Ag maintains its effective antimicrobial status, however restricted to topical use whilst, colloidal AgNps is currently promoted as an alternative medicine treatment for a vast number of non-communicable diseases including DM (Woldu and Lenjisa, 2014). The reasons include its unique and tunable surface plasmon resonance (SPR), decreased side effects, non-toxicity, and ease of biodegradability that seem to possess the ability to decrease blood glucose, lipid levels, inflammation, and increase serum insulin levels and expression using *in vitro* and *in vivo* research methods (Alkaladi et al., 2014). However, the pharmacokinetic implications of these Nps for treatment of different types of diseases require more detailed investigation.

A major component of using phytotherapy such as that belonging to *Ocimum basilicum* (Sweet basil) and *Ocimum sanctum*/*Ocimum tenuiflorum* (Holy basil/Tulsi) from the family Lamiaceae (Kaya et al., 2009) is due to its dynamic effect on the human body, that appears to elicit the same response to currently available antihyperglycaemic drugs, with the exclusion of negative side effects. However, due to their vast bioactive chemical constituents such as, polyphenols, flavonoids, alkaloids, terpenoids, steroids, and glycosides, that synergistically coexist, limits our understanding of their full therapeutic effectiveness (Kaya et al., 2009; Hannan et al., 2015). To address this, functionalizing green AgNps derived from these pharmacologically important plants is a viable option to use for preparation of colloidal drugs, thus enhance the nature of well-known medicinal plants in combination with the different specificities of nanotherapy (Bariyah, 2013). Indeed, it is expected that the enhanced biocatalytic activity of AgNps which contains *in situ* generated capping agents synthesized from the leaf of *O. basilicum*, *O. sanctum* and in combination, may have the capacity to serve as dual antidiabetic and antimicrobial agents.

## 2. Materials and methods

### 2.1. Chemicals and materials

Fresh leaves of *O. basilicum* and *O. sanctum* were collected from Tropical Garden Nursery in KwaZulu Natal, South Africa (SA). The plants were botanically identified in the KwaZulu Natal (KZN) Herbarium Durban, SA by Mr. M.A. Ngwenya and voucher specimens were deposited (Voucher 1: *O. basilicum* L., Det: Malapermal, V.,

NH0137401; Voucher 2: *O. tenuiflorum* (*sanctum*) L., Det: Malapermal, V., NH0137400) and the solvents absolute ethanol obtained from Merck (SA) was of analytical grade. Silver nitrate ($AgNO_3$, ACS reagent), type Vi-B from Porcine α-amylase; *Bacillus stearothermophilus* α-glucosidase; potato starch; p-nitrophenyl-α-D-glucopyranoside (pNPG); 3,5-dinitrosalicylic acid and sodium potassium tartrate were purchased from Sigma–Aldrich Chemicals (SA) and Acarbose, Glucobay® 50 was purchased from a local pharmacy. Gentamycin 10 μg and Vancomycin 30 μg discs were purchased from Davies Diagnostics (SA).

### 2.2. Preparation of crude extracts for enzyme analysis

#### 2.2.1. *O. basilicum* and *O. sanctum* crude extracts

*O. basilicum* and *O. sanctum* crude extracts for the α-amylase and α-glucosidase analysis were prepared by using 10 g each of leaves and flowers that were cleaned, weighed and crushed in a glass beaker. To the respective plant parts 100 ml of 60% EtOH, 70% EtOH and distilled water, respectively were added and left to stand for 24 h. The extract was filtered into a conical flask using a mutton cloth and Whatman No. 1 filter paper. The resultant extract had 10% concentration and was used as a stock solution (Ahmad and Beg, 2001).

#### 2.2.2. *O. sanctum* ethanol based crude extracts

For the α-glucosidase analysis additional extracts for *O. sanctum* leaf parts were used to prepare homoeopathic 150 g mother tinctures. The method used was in accordance with method 2a of the German Homoeopathic Pharmacopoeia (2005); the plant parts were dispensed in 43% m/m (60% v/v EtOH) alcohol and were prepared by maceration. The mixture was then left to stand for not less than 10 days, before eventually being expressed and filtered using mutton cloth and Whatman No. 1 filter paper (German Homoeopathic Pharmacopoeia, 2005).

#### 2.2.3. *O. sanctum* aqueous based crude extracts

In addition, 100 g fresh leaves of *O. sanctum* were homogenized with 10 ml of sterile distilled water, using a mortar and pestle, so that a 100% solution was obtained. This was filtered through a mutton cloth and Whatman No. 1 filter paper (Khogare and Lokhande, 2011).

For all the crude extracts the solvents were allowed to evaporate using a rotary evaporator (Heidolph Rotavac) at a temperature of 40–50 °C until a semi solid sticky mass was obtained. All the extracts were finally freeze dried using a freeze-dryer (Virtis).

### 2.3. Biosynthesis of AgNps

The *O. basilicum* and *O. sanctum* leaf extract was prepared by taking 10 g of thoroughly washed and finely cut leaves in an Erlenmeyer flask in combination with 100 ml of sterile deionised water, the mixture was boiled for 10 min, and then cooled. Briefly, 10 ml of the leaf extract was added drop wise (2 ml) to 45 ml of 1 mM $AgNO_3$ solution and vigorously stirred with the aid of a magnetic stirrer, until the first colour change (brown solution) that indicated the reduction of $Ag^+$ ions after a few minutes. The formation of AgNps was monitored for a period of 36 h. The method was repeated in combination (*O. sanctum* plus *O. basilicum*) to obtain the extract under the above mentioned standard conditions to evaluate the synergistic effect.

#### 2.3.1. Characterization

The AgNps were characterized using UV–Vis spectrophotometer (Varian Cary-50 UV spectrophotometer) linked to a TCC-240A Shimadzu heating vessel temperature controlled cell holder) in the range of 300–700 nm. The particle size and shape were obtained by conducting TEM studies, by placing 1 μl of the samples on formvar coated grids, air dried and viewed at 100 kV (JEOL 1010 TEM using a Megaview III camera and iTEM software). For the particles' images and elemental analysis studies, the samples were prepared by fixing the powder particles to a microscope holder, using conducting carbon tape; and subjected to Carl Zeiss, model EVO HD 15 scanning electron microscope with EDX detector, Oxford Instruments. FTIR spectra were recorded for the green aqueous leaf extract and AgNps with Bruker Alpha FTIR Spectrophotometer. Differential Light Scattering *Malvern Zetasizer Nano ZS* (*Malvern* Instruments Ltd., UK) Merck 2423 instrument was used to measure particle size and zeta potential.

### 2.4. Antidiabetic screening

#### 2.4.1. α-amylase inhibitory test

The effect of time and dose on the inhibitory activity of α-amylase (Type Vi-B from Porcine pancreas) was investigated by methods described by Ali et al. (2006) and Aujla et al. (2012), respectively.

1. Time-dependent method: Briefly, 120 μl of the test sample (3 mg/ml for AgNps and 2 mg/ml for crude extracts) was taken, 480 μl of distilled water and 1200 μl of the potato starch (0.5% w/v primed in 20 mM phosphate buffer) were mixed, 600 μl α-amylase (0.05 g of α-amylase prepared in 100 ml ice-cold distilled water) was added to the reaction mixture and incubated at 25 ± 2 °C for 3 min. After every 1 min, 200 μl was removed from the reaction mixture and 100 μl of DNS colour reagent (96 mM 3,5-dinitrosalicylic acid, 12 g sodium potassium tartrate in 8 ml of 2 M NaOH) was added. The reaction mixture was heated for 15 min at 85 ± 2 °C. After cooling, 900 μl of distilled water was added to the mixture and mixed thoroughly. The optical density (OD) was recorded at 540 nm against the blank. The blank contained 600 μl of distilled water instead of enzyme solution and for the control, test samples were replaced with 120 μl and thus represented maximum enzymatic activity. For $t = 0$ min, a separate experiment was performed, by adding the samples to the DNS solution immediately after addition of the enzyme solution. The assay was performed in triplicate. For calculating the percentage inhibition, the following equations were used. Firstly, the net absorbance (A) using Eq. (1) due to maltose generated was calculated. Secondly, from the net absorbance obtained, the percentage (w/v) of maltose generated was calculated from the Eq. (2) obtained from the equation in the maltose standard calibration curve (0–2% w/v). Finally, the percentage inhibition was calculated at

$t$ = 3 min using Eq. (3) and 50% inhibition or higher was taken as significant ($p < 0.05$).

$$\text{Absorbance at 540 nm control or plant extract} = A_{540\text{nm}}\text{Test} - A_{540\text{nm}}\text{Blank} \quad (1)$$

$$\%\ \text{Reaction} = \frac{\text{Mean maltose in sample}}{\text{Mean maltose in control}} \times 100 \quad (2)$$

$$\%\ \text{Inhibition} = 100 - \%\ \text{Reaction} \quad (3)$$

2. Dose-dependent method: briefly, 1 ml α-amylase (0.5 unit/ml) primed in 20 mM phosphate buffer (pH 6.9) was pre-incubated for 30 min with a 1 ml test solution (0.0002–2 mg/ml). The reaction was started by the addition of 1 ml potato starch (0.5% w/v, prepared by dissolving in 100 ml distilled water). The reaction mixture was incubated at 25 ± 2 °C for 30 min. Finally, the catalytic reaction was terminated with the addition of 1 ml DNS reagent. The reaction mixture was heated for 15 min at 85 ± 2 °C in a water bath. The tubes were cooled to room temperature and 9 ml of distilled water was added. Individual blanks were prepared for amending the background absorbance; colour reagent was added prior to the addition of starch solution and placed into the water bath. For control incubations all procedures were the same except that the AgNps extracts was replaced by 1 ml distilled water. The OD was recorded at 540 nm. Antidiabetic medicine acarbose in concentrations of 0.016–1 mg/ml was used as positive control. The assay was performed in triplicate and the mean absorbance was used to calculate percentage of α-amylase inhibition:

$$I_{\alpha-\text{Amylase}}\% = \frac{(\Delta A540\text{ nm Control} - \Delta A540\text{ nm Sample})}{\Delta A540\text{ nm Control}} \times 100 \quad (4)$$

#### 2.4.2. α-Glucosidase inhibitory test

The α-glucosidase inhibitory test ($I_{\alpha\text{-Glucosidase}}$) was performed by preparing, 0.1 ml of 0.5 unit/ml α-glucosidase prepared in ice-cold distilled water that was pre-incubated with 0.1 ml of test samples (range of 0.2 mg/ml and 0.3 mg/ml) for 5 min. 0.1 ml of the substrate pNPG 3 mM prepared in 0.01 M phosphate buffer (pH 6.9) was added to start the reaction. After further incubation at 37 ± 2 °C for 30 min, the reaction was stopped by adding 1.5 ml of 0.1 M sodium carbonate. Individual blanks were prepared for amending the background absorbance; buffer was added instead of the enzyme. For the control incubations all procedures were the same except that the test extract was replaced by buffer. Antidiabetic medicine acarbose in concentrations of 0.00001–1 mg/ml was used as positive control. Enzymatic activity was quantified by measuring the OD at 405 nm. Percentage α-glucosidase activity is calculated by using the following equation (Nguyen et al., 2011):

$$I_{\alpha-\text{Glucosidase}}\% = \frac{(\Delta A540\text{ nm Control} - \Delta A540\text{ nm Sample})}{\Delta A540\text{ nm Control}} \times 100 \quad (5)$$

#### 2.4.3. $IC_{50}$ values of active AgNps extracts

The potency of AgNps extracts as inhibitors of enzyme catalytic activities of both α-amylase and α-glucosidase was assessed in terms of their $IC_{50}$ values (inhibitor concentration that reduces enzyme activity by 50%) (Cheng and Prusoff, 1973; Mogale et al., 2011). Briefly, aliquots of α-amylase and α-glucosidase enzymes were pre-incubated with increasing concentrations of the AgNps extracts and acarbose. Catalytic reactions were started, terminated and enzyme activities determined as mentioned above. The activity of fractions and compounds was assessed by plotting percentage inhibition against a range of concentrations and determining the inhibitory concentration 50% ($IC_{50}$) value by interpolation of a cubic spline dose–response curve using GraphPad Prism® 5.03 software.

#### 2.4.4. Inhibition kinetics of α-amylase and α-glucosidase

Mode of inhibition of AgNps on enzyme activity was determined as described by Ali et al. (2006). Briefly, fixed amounts of both α-amylase and α-glucosidase were incubated with increasing concentrations of starch and pNPG, respectively at 37 ± 2 °C for 20 min, in the absence and presence of the AgNps extracts (3 mg/ml). Reactions were terminated and absorption measurements carried out as mentioned above. The amount of products, reducing sugars as maltose and p-nitrophenol respectively, that are liberated were determined from the corresponding standard curve and then converted to reaction velocities.

### 2.5. Antibacterial screening

Mueller Hinton agar was seeded with appropriate well mixed overnight nutrient broth culture of each test microorganism to 0.5 McFarland turbidity standard: *Staphylococcus aureus* (ATCC 25923), *Escherichia coli* (ATCC 26922), *Pseudomonas aeruginosa* (ATCC 27853), *Salmonella* species (UKQC 9990), and *Bacillus subtilis* (ATCC 6051), respectively. $1 \times 10^6$ colony forming units (CFU) per millilitre was used, by streaking evenly on to the surface of the medium with a sterile cotton swab to allow for even growth. Wells were cut from the agar plates using a sterile bore (Sivaranjani and Meenakshisundaram, 2013). The wells were loaded with 30 µl for each sample using a sterile micropipette allowing a 10 min diffusion time. Vancomycin 30 µg, Gentamycin 10 µg discs, and 1 mM $AgNO_3$ were used as positive controls and distilled water served as the negative control. The plates were incubated at 37 ± 2 °C for 24 h thereafter the plates were examined for any clearing zones around the walls and/or discs. The zones of inhibition were measured in mm using a measuring ruler and compared to the controls. This experiment was carried out six times for confirmation and statistical analysis.

### 2.6. Statistical analysis

The statistical analysis of data was expressed as mean ± standard error of the mean (SEM). The antibacterial study were analysed using the Wilcoxon Signed Ranks test and the antidiabetic study were analysed by means of a one-way and a two-way Anova and Bonferroni multiple comparison post test using the GraphPad Prism® 5.03 software.

Please cite this article in press as: Malapermal, V. et al., Enhancing antidiabetic and antimicrobial performance of *Ocimum basilicum*, and *Ocimum sanctum* (L.) using silver nanoparticles. Saudi Journal of Biological Sciences (2015), http://dx.doi.org/10.1016/j.sjbs.2015.06.026

## 3. Results

### 3.1. GC–MS studies

The phytochemical examination of *O. basilicum* typically includes the presence of tannins, steroids, terpenoids, flavonoids, cardiac glycosides (El-Beshbishy and Bahashwan, 2012; Usman et al., 2013) squalene, phenol,2-methoxy-4-(1-propenyl)-[Isoeugenol], caryophyllene oxide, nonadecane, decane,2,9-dimethyl-, linolenic acid ethyl ester, hexadecanoic acid ethyl ester (Jaiganesh et al., 2012), linalool, 1,8-cineole, borneol, eugenol, and α-caryophyllene (Usman et al., 2013). Whereas in previous studies from a comparative perspective, the crude extract composition of *O. sanctum* appears to be marginally different, with a varied concentration of alkaloids, tannins, glycosides, saponins, terpenoids, tri-terpenoids, steroids, flavonoids (Joshi et al., 2011; Sudha et al., 2011), ascorbic acid, carotene, polyphenols, fatty acids and sitosterol, sugars (xylose and polysaccharides), pectins, sesquiterpene and monoterpenes. Some of these phytochemicals are believed to be responsible for the high therapeutic potency of *O. sanctum* including, hypoglycaemic and antibacterial effects of (Govind and Madhuri, 2010; Joshi et al., 2011), anticataleptic, antitoxic, immunomodulatory, analgesic, cardioprotective and anticancer properties (Bariyah, 2013).

In the present study, the chemical composition of the leaf extract of *O. basilicum* and *O. sanctum* (L.) was determined via GC–MS analysis using Shimadzu GC-2010 Plus with GCMS-QP2010SE equipped with a split/splitless capillary injection port. The capillary column used was a GL Sciences InertCap 5MS/Sil Length 30 mm, I.D. 0.25 mm, file thickness 0.25 μm. Chemical constituents were identified after comparison with those available in the computer library (NIST) attached to the GC–MS instrument. The organic compounds that were identified in *O. basilicum* leaf extract include: cyclohexanol; menthol; hexanedioic acid/adipic acid; 3,7,11,15-tetramethyl-2-hexadecen-1-ol; 13-methyl-14-pentadecene-1,13-diol; and terpenes such as squalene and phytol consistent with those previously published (Lee et al., 2005). The GC–MS report for *O. sanctum* recorded phenolics, terpenes (linalool, beta-terpeneol, phytol, squalene), terpenoids (camphor), and various amine compounds, similar to previous reports (Kothari et al., 2004) (Tables S1 and S2). In the present study, the variability in chemical composition of the two plants could depend on the selection of extractant, extraction techniques (Eloff, 1998), climatic and geographical conditions (Saha et al., 2013).

### 3.2. Characterization tests of the AgNps

#### 3.2.1. UV–Visible studies

The synthesis of AgNps with various leaf extracts was successful; the nanometallic silver exhibited a well-defined absorption peak at 438 nm from *O. basilicum*, 439 nm for *O. sanctum*, and 433 nm from the combination extract. The consequent colour changes were observed from a light yellow to a brown colour (Fig. 1(A–C)). The interaction of Nps with biomolecules of *O. basilicum* leaf, *O. sanctum* leaf and in combination *O. sanctum* + *O. basilicum*, respectively validated the reduction of $Ag^+$ ions to $Ag^0$ by the secondary plant metabolites that are in turn oxidized to other species. Even though the mechanism has not been adequately elucidated, it is components such as polyols, amines, phenolics, flavonoids, and water-soluble heterocyclic compounds as well as other factors such as reducing sugars, proteins and other oxido-reductive labile metabolites present in the *O. basilicum* and *O. sanctum* leaf extracts that possess the ability to reduce $Ag^+$ ions to $Ag^0$. Similar UV–Vis spectrum results have been ascertained in the case of the stabilizing effect of natural biological extracts in the formation of stable metal Nps (Raman et al., 2012; Rao et al., 2013; Kotakadi et al., 2014).

#### 3.2.2. TEM analysis

The results obtained from the TEM monograph indicated the size and shape properties of the formed AgNps derived from *O. sanctum*, *O. basilicum* respectively, and in combination. Representative TEM images indicated that most of the particles were near spherically shaped and were predominantly monodispersed (Ahmad et al., 2010). The particles exhibited a distribution of mean size ± standard deviation (SD), at a size range of 17.0 ± 8.94 nm for *O. basilicum* AgNps, 15.0 ± 12.34 nm for *O. sanctum* AgNps and 17.0 ± 8.44 nm for the combination *O. sanctum* + *O. basilicum* AgNps (Figs. S1 and S2). These results show that it is possible to prepare stable AgNps of size less than 17 nm by varying the ratio of $AgNO_3$, *O. sanctum*, *O. basilicum* and use a combination of extract solutions from two different plants as a means for effective production of stable AgNps.

#### 3.2.3. SEM–EDX analysis

The crystalline nature of AgNps and nanosize was confirmed by the SEM and EDX patterns. The SEM image showed relatively spherical shaped Nps formed with a diameter range of 100 nm. The EDX revealed a strong signal in the silver region at five different areas for all three samples, and thus confirmed the formation of AgNps. In addition, an observed spectral signal for oxygen (O) and other elements indicated the extracellular organic moieties (originating from *O. basilicum* and *O. sanctum* leaf extracts, respectively) that were adsorbed on the surface or in the vicinity of the metal nanoparticles or may originate from the biomolecules that were bound to the surface of the Nps. Peaks for sulphur (S), phosphorus (P) and nitrogen (N) correspond to the protein capping over the AgNps. However, certain elements come from the artefact during sample preparation. Peaks for carbon (C) originate from the grid used (Figs. S3 and S4).

#### 3.2.4. Zeta Potential and DLS analysis

DLS measurement presented the size distribution of the Nps with an average size of 56.81 nm and stability for the AgNps *O. basilicum* at −19.8 mV; for AgNps *O. sanctum* at size of 467.4 nm and stability at −23.3 mV; and for AgNps *O. sanctum* + *O. basilicum* at size of 155.1 nm and stability at −24.3 mV in zeta potential analysis. Unavoidably, the particle size obtained from TEM, SEM–EDX and DLS is different, due to the varying principles used for measurement, similar observations were reported for AgNps prepared from *Melia azedarach* (Raman et al., 2012). However, a stable size dispersion of particles was evident from the zeta potential, a zeta potential higher than +30 mV or lesser than −30 mV is indicative of a stable system (Kotakadi et al., 2014) (Fig. S5). Many reports have proposed that surface active molecules can stabilize the Nps and that the reaction of the metal ions is possibly

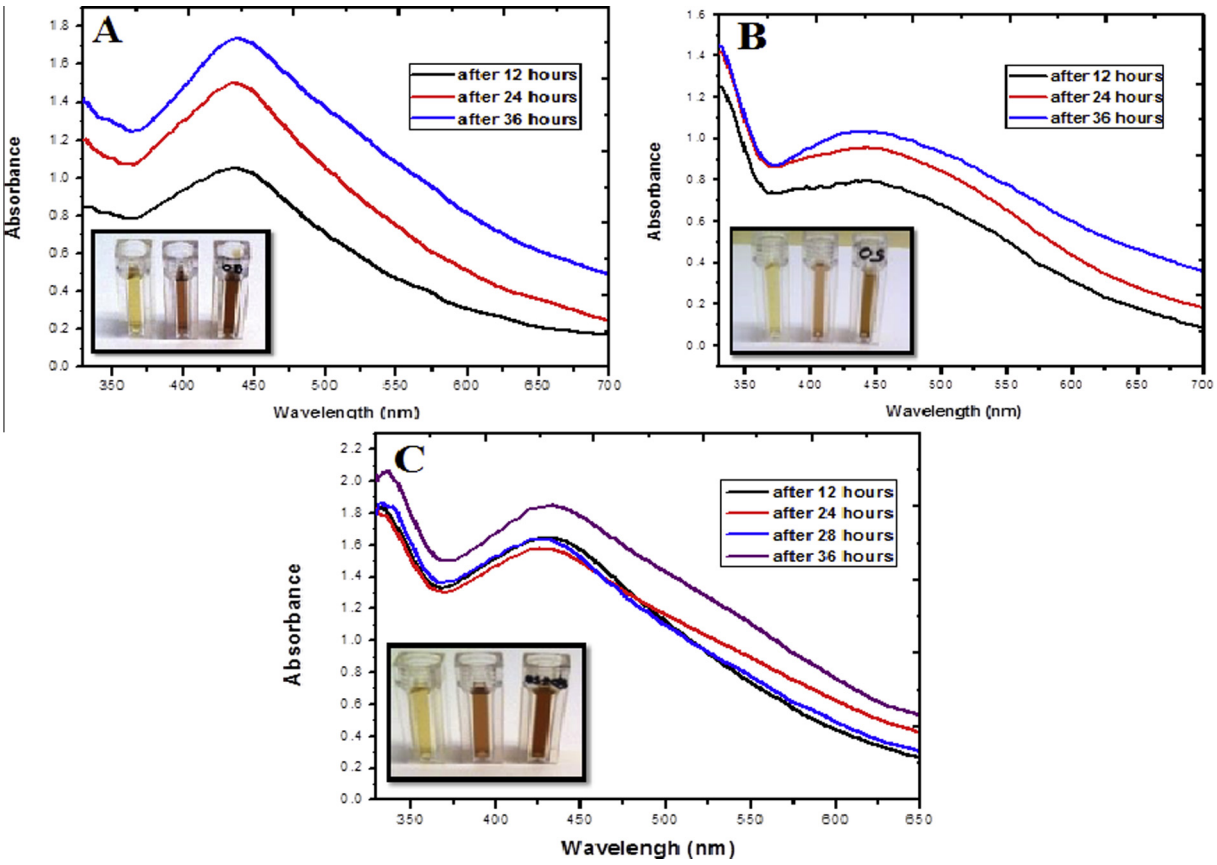


**Figure 1** UV–Visible absorption spectra of AgNps synthesized using (A) aq. *O. basilicum* leaf extract (B) aq. *O. sanctum* leaf extract (C) aq. *O. sanctum* in combination with *O. basilicum* leaf extract at different reaction times. Progressive colour change indicating the formation of AgNps over a 36 h period; from L → R AgNps formation over 12 → 24 → 36 h.

facilitated by reducing sugars and or terpenoids (Song and Kim, 2009). In addition, organic molecules such as carotenoids, vitamins, minerals, amino acids, sterols, glycosides, alkaloids, flavonoids, terpenes and phenolics can also act as surface active molecules responsible for stability and formation of the AgNps (Huang et al., 2007).

### 3.2.5. FTIR studies

FTIR was used to identify any potential biomolecules, present in the leaf extract (*O. sanctum* and *O. basilicum*), which are responsible for reducing $Ag^+$ ions to $Ag^0$. FTIR spectra of the crude aq. extract and AgNps derived from *O. basilicum* showed a decrease in stretching frequency from 3300.21 to 3297.12 $cm^{-1}$ suggesting an OH functional group. Furthermore a shift from 1634.78 to 1635.67 $cm^{-1}$ is assigned to the carbonyl C═O stretch, whereas peaks at 1217 $cm^{-1}$ can be attributed to the ether linkages (Fig. 2(A)). For *O. sanctum* similar results obtained to that of *O. basilicum* with the exception of C═O bond that was identified (Fig. 2(B)). The dual properties of AgNps synthesized from *O. basilicum* and *O. sanctum* were evident with the addition of C–H stretch (Fig. 2(C)). It is thus speculated that the conversion of C–OH biomolecules to C═O group may be responsible for the reduction of $Ag^+$ to $Ag^0$. The absorption peak at 1635.48–1635.82 $cm^{-1}$ for AgNps (*O. sanctum*) may be assigned to the amide I bond or proteins arising due to carbonyl stretch, suggesting that the proteins are interacting with biosynthesized Nps and that their secondary structure was not affected during reaction with $Ag^+$ ions or after binding with AgNps. These IR spectroscopic studies confirmed that a carbonyl group of amino acid residues has a strong binding ability with the metal suggesting the formation of a layer covering the metal Nps and acting as a capping agent to prevent agglomeration and providing stability to the medium. The range of 3250–3400 $cm^{-1}$, that is, amide region from the earlier literature states that binding as well as stabilization takes place by free amide groups present in proteinaceous substances used for synthesis (Kumari et al., 2015). Supported by the GC–MS results, N–H amide compounds were identified from *O. sanctum* leaf extract, these results confirm the presence of possible proteins acting as reducing and stabilizing agents, namely: Cis-11-Eicosenamide, 8-Methyl-6-nonenamide, 13-Docosenamide, (13z)-N-([(13z)-13-Docosenoylamino]methyl)-13-docosenamide. Thus, a mechanism for the biosynthesis of AgNps can be elucidated using amide compounds identified from *O. sanctum* extracts which acts as a natural reducing agent (Scheme 1(A)). Peak at 3100–3300 $cm^{-1}$ is assigned to O–H stretching in alcohols and phenolic compounds, the results are similar to previous reports (Singhal et al., 2011). Previous reports indicate peaks for *Ocimum*

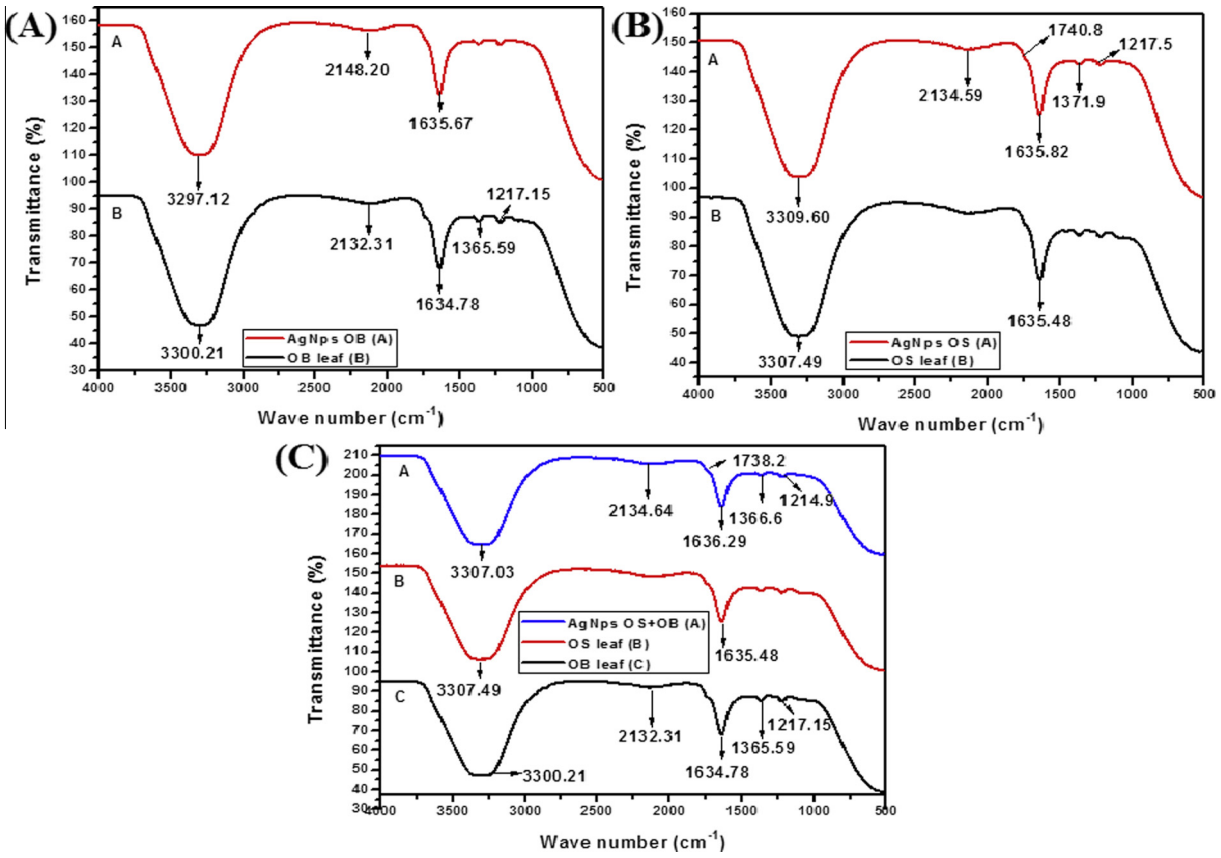


**Figure 2** FTIR spectra of AgNps synthesized using (A) aq. *O. basilicum* leaf extract (B) aq. *O. sanctum* leaf extract (C) aq. *O. sanctum* in combination with *O. basilicum* leaf extract.

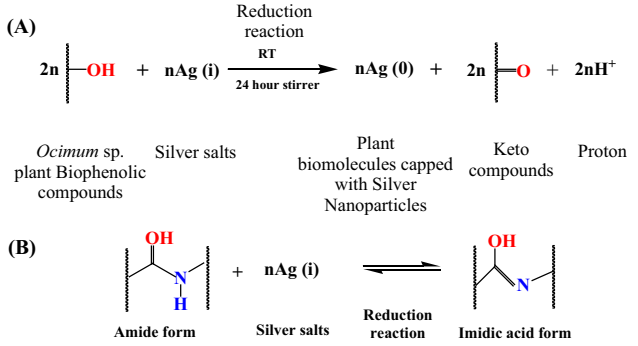


**Scheme 1** Proposed mechanism was elucidated using (A) phenolic compounds present in abundance in *Ocimum* sp. for the rapid formation of medicinal AgNps (B) amide compounds typically identified in *O. sanctum* leaf extracts for the rapid formation of medicinal AgNps.

sp. are more characteristic of eugenol, linalool and terpenes that are abundant in these plant extracts (Ramteke et al., 2013). Depending on the above observation, it can be assumed that the stabilization and formation of AgNps are achieved by the phenolic as well as aromatic compounds present in the *O. sanctum* and *O. basilicum* extracts (Scheme 1(B)).

### *3.3. Inhibitory effect of AgNps on α-amylase and α-glucosidase activity*

Table 1 shows the percentage inhibition and $IC_{50}$ values obtained for the AgNps synthesized from *O. basilicum*, *O. sanctum* and their respective crude extracts. AgNps synthesized from *O. sanctum* and *O. basilicum*, respectively demonstrated high inhibitory activity against α-amylase than acarbose, however, the crude *O. sanctum* and *O. basilicum* extracts demonstrated greater inhibition compared to acarbose (Fig. S6). Table 2 shows the inhibition against *B. stearothermophilus* α-glucosidase of the AgNps synthesized from *O. sanctum* (89.31 ± 5.319%) and *O. basilicum* (79.74 ± 9.51%) indicating the activity was far greater compared to that of acarbose and their respective crude extracts. However, the combination derived AgNps extract yielded the lowest inhibitory activity (29.03 ± 15.92%) against α-glucosidase compared to acarbose, *p*-value 0.05 (Fig. S7). The enzyme kinetics revealed inhibition in a competitive manner for AgNps derived from *O. sanctum* leaf extract on α-amylase ($K_m$ is increased, whereas $V_{max}$ remain the same). These findings indicate that some of the α-amylase inhibitory components in AgNps derived from *O. sanctum* aq. extract may be structural analogues of the substrate that compete for binding at the active site of α-amylase. The case of AgNps derived from *O. basilicum* leaf extract on α-amylase was found to be uncompetitive ($K_m$ is decreased and $V_{max}$ is decreased) this suggests that some of the α-amylase

**Table 1** Inhibitory effect of AgNps and crude extracts on α-amylase activity.

| Samples | *In vitro* α-amylase inhibition % 3 mg/ml (AgNps) 2 mg/ml (crude extracts) | *p*-value | $IC_{50}$ (mg/ml) [a]0.05–1.6 mg/ml [b]0.002–2 mg/ml [c]0.003–3 mg/ml |
|---|---|---|---|
| Acarbose | 48.27 ± 1.79 | < 0.0001 | 0.022 |
| AgNps OS | 59.57 ± 3.72* | 0.004 | 0.070[a] |
| AgNps OB | 59.79 ± 6.91 | 0.013 | 0.016[a] |
| AgNps OS + OB | 54.94 ± 6.56 | 0.014 | 0.169[a] |
| OS Aq. dist. (leaf) | 61.23 ± 5.24 | 0.007 | 0.028[b] |
| OS 60% EtOH (leaf) | 66.33 ± 4.26* | 0.004 | 0.021[b] |
| OS 70% EtOH (leaf) | 64.14 ± 13.47 | 0.018 | 0.017[c] |
| OB Aq. dist. (leaf) | 61.23 ± 5.24 | 0.007 | 0.029[b] |
| OB 60% EtOH (leaf) | 55.13 ± 9.17 | 0.027 | 0.033[b] |
| OB 70% EtOH (leaf) | 55.81 ± 7.86 | 0.019 | 0.009[c] |

Results are expressed as mean ± SEM; $N = 3$; $p < 0.05$, *p*-value summary * vs control; OS = *O. sanctum*, OB = *O. basilicum*.

**Table 2** Inhibitory effect of AgNps and crude extracts on α-glucosidase activity.

| Samples | *In vitro* α-glucosidase inhibition % [a]0.2 mg/ml [b]0.3 mg/ml | *p*-value | $IC_{50}$ (mg/ml) [c]0.0003–3 mg/ml [d]0.0002–0.2 mg/ml |
|---|---|---|---|
| Acarbose | 73.75 ± 12.86 | 0.002 | 0.001 |
| AgNps OB[b] | 79.74 ± 9.51 | 0.014 | 1.533[c] |
| AgNps OS[b] | 89.31 ± 5.32 | < 0.0001 | 0.009[c] |
| AgNps OS + OB[b] | 29.03 ± 15.92 | – | NI |
| OS Aq. dist. (leaf)[b] | 62.25 ± 11.25 | 0.012 | 0.089[c] |
| OS 60% EtOH (leaf)[a] | 49.50 ± 2.18 | 0.0002 | 2.566[d] |
| OS 70% EtOH (leaf)[b] | 66.00 ± 7.80 | 0.004 | 0.288[c] |
| OB Aq. dist. (leaf)[b] | 34.75 ± 3.705* | 0.003 | 10.55[c] |
| OB 60% EtOH (leaf)[b] | 50.50 ± 3.594 | 0.001 | 0.002[c] |
| OB 70% EtOH (leaf)[b] | 69.89 ± 6.871 | < 0.0001 | 0.007[c] |

Results are expressed as mean ± SEM; $N = 3$; $p < 0.05$, *p*-value summary * vs control; OS = *O. sanctum*; OB = *O. basilicum*; NI = No Inhibition.

inhibitory components in this AgNps bind only to the enzyme-substrate complex and may distort the active site. Both *O. sanctum* and *O. basilicum* derived AgNps appeared to be in competitive inhibition on α-glucosidase activity. In view of the α-glucosidase effects of AgNps synthesized from *O. sanctum* and *O. basilicum* this may be comparable to the effect of the standard α-amylase and α-glucosidase inhibitor, acarbose, which competitively and reversibly inhibits α-glucosidase enzyme from the intestine and the pancreas (Kim et al., 1999). Due to the fact that the EtOH (70%) leaf *O. basilicum* and *O. sanctum* extracts showed highest percentage inhibition against α-glucosidase their modes of inhibition were determined. The natural *O. sanctum* extract appeared to be a close competitive inhibitor and *O. basilicum* natural extract appeared to show inhibition in an uncompetitive manner against α-glucosidase activity. As a result, the catalytic hydrolysis reaction using *in vitro* α-amylase and α-glucosidase as a means of evaluation (Bernfeld, 1955) suggested a varied MOA presented in the reaction mechanism by the crude phytocompound–enzyme mixture in comparison to the metal-Np-enzyme composite, which may be due to the variation in the two enzymes structural and catalytic properties.

### 3.4. Antimicrobial activity

Table 3 depicts the antibacterial activity of AgNps *O. sanctum* at (6.333 ± 1.174) against *S. aureus*, *p*-value 0.713 and inhibition for AgNps *O. basilicum* (3.667 ± 0.333), *p*-value 0.026, whereas, combination extracts showed the lowest antibacterial activity compared to Vancomycin (6.000 ± 0.000), *p*-value 0.027. Antimicrobial properties of AgNps *O. sanctum* were observed against *E. coli* (6.000 ± 1.033), *p*-value 0.518, followed by *P. aeruginosa* (3.167 ± 0.601), *p*-value 0.038, and the least was noticed against *Salmonella* sp. (2.000 ± 0.000), *p*-value 0.014 as shown in Figs. S8–S10, a similar report was obtained on *O. sanctum* AgNps synthesized via the green route, and were found to be highly toxic against clinically isolated bacterial species (Rout et al., 2012). The highest antibacterial activity was observed against *E. coli* (4.167 ± 0.792), *p*-value 0.339 using AgNps synthesized from *O. basilicum*, and the lowest was observed against *P. aeruginosa* (2.667 ± 0.333), *p*-value 0.026, similar to results obtained in previous research (Sivaranjani and Meenakshisundaram, 2013). However, no activity was observed against *Salmonella* sp. The combined extracts AgNps displayed the lowest

**Table 3** Zones of inhibition in (mm) for AgNps against the various bacterial test strains.

| Samples | *B. subtilis*[a] | *E. coli*[a] | *P. aeruginosa* [a] | *Salmonella* sp. [a] | *S. aureus*[a] | *S. aureus*[b] |
|---|---|---|---|---|---|---|
| AgNps OS | 2.000 ± 0.000 | 6.000 ± 1.033 | 3.167 ± 0.601 | 2.000 ± 0.000 | 6.333 ± 1.174 | 2.667 ± 0.333 |
| AgNps OB | 2.000 ± 0.000 | 4.167 ± 0.792 | 2.667 ± 0.333 | NI | 3.667 ± 0.333 | 1.333 ± 0.333 |
| AgNps OS + OB | 3.000 ± 0.000 | 1.500 ± 0.224 | 2.000 ± 0.365 | NI | 2.167 ± 0.477 | 1.000 ± 0.000 |
| OS 10% aq. extracts. | NI | NI | NI | NI | NI | NI |
| OB 10% aq. extracts. | NI | NI | NI | NI | NI | NI |
| OS + OB 10% aq. extracts | NI | NI | NI | NI | NI | NI |
| Control (1 mM $AgNO_3$) | 2.000 ± 0.000 | 1.500 ± 0.224 | 2.000 ± 0.000 | 1.667 ± 0.211 | 2.000 ± 1.095 | 2.333 ± 0.333 |
| +Control (Gentamycin 10 μg) | 10.000 ± 0.000 | 5.000 ± 0.000 | 6.000 ± 0.000 | 4.000 ± 0.000 | – | – |
| +Control (Vancomycin 30 μg) | – | – | – | – | 6.000 ± 0.000 | 3.000 ± 0.000 |
| −Control (distilled water) | NI | NI | NI | NI | NI | NI |

Results are expressed as mean inhibition ± SEM, $N = 6$; OS = *O. sanctum*, OB = *O. basilicum*; NI = No Inhibition.
[a] Grouping variable: 100 μl of bacteria per plate.
[b] Grouping variable: 200 μl of bacteria per plate.

antimicrobial properties and the crude 10% aq. extracts showed no inhibitory activity against the test strains. The wide range of particle sizes, specifically 3–17 nm with a narrow size distribution were obtained from the two different plants. Nps with sizes <15 nm exhibited in the Minimum Inhibitory Concentration (MIC) and Minimum Bactericidal Concentration (MBC) tests, for 1 in 2 dilution of AgNps *O. sanctum* against *Salmonella* sp. was 66.67% no growth (×4 plates) and 33.33% growth when compared to the 100% growth for the water control. MIC and MBC for 1 in 4 dilution of AgNps *O. sanctum* against *Salmonella* sp. were 50% no growth (×3 plates), and 50% growth when compared to the 100% growth for the water control, *p*-value summary 0.045. MIC and MBC for 1 in 2 dilution AgNps *O. sanctum* against *S. aureus* were 100% no growth (×6 plates) and 0% growth when compared to the 100% growth for the water control. However, 17 nm size particles for *O. basilicum* leaf synthesized AgNps against *S. aureus* showed 83.33% no growth (×5 plates) and 16.67% growth; and combination extracts (*O. sanctum* + *O. basilicum*) synthesized AgNps represented 50% no growth (×3 plates) and 50% growth when compared to 100% growth for the water control, *p*-value 0.0003 (Fig. S11).

## 4. Discussion

Current global interest in the use of eco-friendly and economical resources propels the use of highly acclaimed medical plants to direct the green synthesis of metal Np entities, that possess diverse biological and catalytic properties. Furthermore, the rationale for the synthesis of AgNps was twofold: (1) to combine AgNps (higher bioactive properties) with a natural *Ocimum* sp. extracts (chemically inert and less toxicity), and (2) increase the surface phenomenon in the reduction reaction (higher surface to volume ratio) to achieve greater biological activity. Stable spherical colloidal AgNps were synthesized using antidiabetic and antimicrobial potent *O. basilicum* and *O. sanctum* as the reducing agent as opposed to high thermal conversion energy, or hazardous solvents. Inert, spherical Nps with a size range of 3–25 nm were characterized by UV–Vis spectroscopy, TEM, SEM–EDX and stability confirmed by DLS and zeta potential. In addition, important medicinal functional groups were confirmed via FTIR and GC–MS. Inhibitors of α-amylase and intestinal α-glucosidase enzymes retard the rate of carbohydrate digestion, thereby provides an alternative therapeutic option for modulation of postprandial hyperglycaemia (PPHG) (Subramanian et al., 2008). In diabetic patients, a sustained reduction of hyperglycaemia is shown to decrease the risk of developing microvascular and macrovascular diseases and their associated complications (Patel et al., 2012). The results obtained in this study are coherent with previous studies confirming the hypoglycaemic properties of natural *O. basilicum* (El-Beshbishy and Bahashwan, 2012) and *O. sanctum* extracts (Chattopadhyay, 1993) prepared using a variety of extraction techniques (thermal/high energy conversion), hazardous solvents and high dosages. Both the plants exhibited higher inhibitory activity towards the enzymes as opposed to many other hypoglycaemic plants reported in previous studies (Mukherjee et al., 2006). In comparison, first time *in vitro* hypoglycaemic assessment of AgNps synthesized via the green protocol using *Ocimum* sp. indicates higher bioactive properties. The enhanced activity of AgNps obtained in the α-glucosidase assessment may be due to their high surface area to volume ratio, thus increasing the surface area phenomenon (promoting the electron transfer reaction) and may increase the pharmacokinetics from a biological view. The effects of oral hypoglycaemic drugs depend on a number of pharmacokinetic factors such as absorption, metabolism and excretion, and the actions of drugs begin inside the cells, it is believed that AgNps small size are easily carried across the cell membrane by transport proteins and may exhibit prolonged effects in bio-systems (Karthick et al., 2014). Therefore, it is suggested colloidal AgNps to be used as effective nanomedicine for treatment of DM; however, further *in vivo* pharmacokinetic studies are encouraged. Diabetic induced infections are currently increasing at an alarming rate, adding to the associated complications, worsening the effects of the disease and are rapidly draining health care resources (Reid et al., 2012; Tudhope, 2008). Diabetic peripheral neuropathy (polyneuropathy) among all of the other associated co-morbid diabetic conditions is reported to be the prime factor involved in the bacterial aetiology of diabetic foot trauma and ulceration. Upon the initial exposure of a bacterial infection, it is associated with delayed recognition of symptoms combined with poor peripheral circulation that delays healing and encourages opportunistic infection (Shankar et al., 2005). Infectious agents can lead to the worst outcomes in diabetic patients as it can cause gangrene, which may lead to amputation of the foot or limb and even death if prompt treatment is

not ensured. In addition, polymicrobial infections caused by a combination of bacteria such as *Staphylococcus*, *E. coli*, *P. aeruginosa*, and/or MRSA in diabetic foot infections are increasingly becoming a problem, especially in previously hospitalized patients (Hall et al., 2011). In the current study, the green synthesis of AgNps capped with important plant phytochemicals such as phenolics (McCue and Shetty, 2004), flavonoids, carbohydrates, tannins, quinones and other important bioactive compounds (Lokina et al., 2014) contribute to the enhanced properties of the phytochemical mixture with metal Nps. This is especially significant to overcome antimicrobial resistance with greater beneficial outcomes at a lower toxicity to the human body (Lokina et al., 2014). The bactericidal properties of the most exploited AgNps of typically $<20$ nm in diameter can be explained by the release of reactive and charged silver ions from particles (Rout et al., 2012), causing bacterial cell damage in two ways. Either by adhering to the bacterial cell wall, causing disruption in cell-wall permeability and cellular respiration (Singhal et al., 2011), or causing damage by interacting with phosphorus and sulphur containing compounds such as deoxyribonucleic acid (DNA) and proteins (Krishnamoorthy and Jayalakshmi, 2012).

Various AgNps synthesized from *Ocimum* sp. displayed significant antibacterial potency at very low concentration. The small sizes ($<15$ nm) of the Nps play a central role in the interaction and penetration with the bacterial cells and exhibited higher antimicrobial activity than larger Nps (Morones et al., 2005). In addition, indicates a clear distinction in the destruction of Gram negative and Gram positive bacteria specifically the charge they carry, and the variation in cell wall composition (Mubarak et al., 2011). Previous reports indicate that the electrostatic attraction between negatively charged bacterial cells and positively charged Nps or vice versa is crucial for the bactericidal activity of Nps (Sondi and Salopek-Sondi, 2004). In the current study, AgNps are negatively charged confirmed by the zeta potential analysis, therefore the mechanism of interaction between these particles and the outer membrane of Gram positive bacteria that consist of lipoteichoic acid and teichoic acid showed higher inhibition against *S. aureus*. In comparison, Gram negative bacteria that consist of lipopolysaccharide and an outer membrane remains unclear, however, it would appear that despite the negative surface charge on *E. coli*, *P. aeruginosa*, and *Salmonella* sp. the AgNps may react with the building elements of the bacterial membrane, causing structural changes, degradation and finally cell death (Losasso et al., 2014). However they may be limited by different physiochemical properties of plant molecules capping the surface of the metal Np. Thus, a dose dependent effect of AgNps (in the size range of $<15$ nm) on the Gram negative bacteria is recommended for further studies. Furthermore, coupling the inherent medicinal properties of *Ocimum* sp. with that of AgNps proved to be beneficial to minimize the dose needed to be administered for total antimicrobial reduction against diabetic related pathogens *S. aureus*, *E. coli*, *P. aeruginosa*, *B. subtilis*, and *Salmonella* sp.

## 5. Conclusion

In this study, an environmentally benign, straightforward, facile, and medicinally active phytochemical route synthesized colloidal AgNps from the leaves of indigenous plants found in abundance in SA, *O. basilicum*, *O. sanctum* respectively, and for the first time in combination in an attempt to develop anti-hyperglycaemic agents that elicit a euglycaemic response. These AgNps were characterized by the following techniques, viz., GC–MS, FTIR, UV–Vis spectroscopy, SEM–EDX, TEM, DLS, and zeta potential. The bio-derived AgNps showed excellent inhibitory enzymatic activity/antibacterial properties than their respective crude extract and the standard controls. These observations, plus evidence of their potent antioxidant activity from phenolic rich plants such as *Ocimum* sp. indicate the value of further studies. Thus, synthesis of AgNps based drugs with greater targeted activity coalesced with medicinal phytochemicals derived from the leaves of *O. basilicum* and *O. sanctum* or combined may result in unprecedented opportunities directed at the discovery of a cheaper and more beneficial therapy for hyperglycaemia, and prevention of diabetic induced complications such peripheral neuropathy that predisposes bacterial infections.

## Acknowledgements

Sincere gratitude to Professor R.M. Gengan and Dr. K. Anand for UV/Vis/FTIR Spectrophotometers (Organic Synthesis, Green Chemistry Research Lab, Department of Chemistry, Durban University of Technology (DUT)), Mr. A. Ramsaroop for SEM–EDX (Department of Mechanical Engineering, DUT), Mr. N.K. Broomhead for GC-MS analysis (Department of Chemistry, University of KwaZulu Natal), and thanks to the Research and Postgraduate support DUT – South Africa for funding this project.

## Appendix A. Supplementary data

Supplementary data associated with this article can be found, in the online version, at http://dx.doi.org/10.1016/j.sjbs.2015.06.026.

## References

Ahmad, I., Beg, A.Z., 2001. Antimicrobial and phytochemical studies on 45 Indian medicinal plants against multi-drug resistant human pathogens. J. Ethnopharmacol. 74, 113–123.

Ahmad, N., Sharmab, S., Alama, M.K., Singh, V.N., Shamsid, S.F., Mehtac, B.R., Fatmae, A., 2010. Rapid synthesis of silver nanoparticles using dried medicinal plant of basil. Colloids Surf. B 81, 81–86.

Ali, H., Houghton, P.J., Soumyanath, A., 2006. α-Amylase inhibitory activity of some Malaysian plants used to treat diabetes with particular reference to *Phyllanthus amarus*. J. Ethnopharmacol. 107, 449–455.

Alkaladi, A., Abdelazim, A.M., Afifi, M., 2014. Antidiabetic activity of zinc oxide and silver nanoparticles on streptozotocin-induced diabetic rats. Int. J. Mol. Sci. 15, 2015–2023.

Aujla, M.I., Ahmed, D., Khair-Ul-Bariyah, S., 2012. Comparative analysis of *Ocimum basilicum* and *Ocimum sanctum*: extraction techniques and urease and alpha-amylase inhibition. Pak. J. Chem. 2, 134–141.

Avery, M.A., Mizuno, C.S., Chittiboyina, A.G., Kurtz, T.W., Pershadsingh, H.A., 2008. Type 2 diabetes and oral antihyperglycemic drugs. Curr. Med. Chem. 15, 61–74.

Bariyah, S.K., 2013. An extensive survey of the phytochemistry and therapeutic potency of *Ocimum sanctum* (Queen of Herbs). Pak. J. Chem. 3, 8–18.

Bernfeld, P., 1955. Methods in Enzymology 1. Available: <http://www.sigmaaldrich.com/technical- documents/ protocols/ biology/ enzymatic-assay-of-a-amylase.html> (accessed 04/11/2012).

Bouwmeester, H., Dekkers, S., Noordam, M.Y., Hagens, W.I., Bulder, A.S., De Heer, C., Ten Voorde, S.E., Wijnhoven, S.W., Marvin, H.J., Sips, A.J., 2009. Review of health safety aspects of nanotechnologies in food production. Regul. Toxicol. Pharmacol. 53, 52–62.

Chattopadhyay, R.R., 1993. Hypoglycemic effect of *Ocimum sanctum* leaf extract in normal and streptozotocin diabetic rats. Indian J. Exp. Biol. 31, 891–893.

Cheng, Y., Prusoff, W.H., 1973. Relationship between the inhibition constant (KI) and the concentration of inhibitor which causes 50 percent inhibition (I50) of an enzymatic reaction. Biochem. Pharmacol. 22, 3099–3108.

Cryer, P.E., 2008. Hypoglycemia: still the limiting factor in the glycemic management of diabetes. Endocr. Pract. 14, 750–756.

Ehdaie, B., 2007. Application of nanotechnology in cancer research: review of progress in the National Cancer Institute's Alliance for Nanotechnology. Int. J. Biol. Sci. 3, 108.

El-Beshbishy, H., Bahashwan, S., 2012. Hypoglycemic effect of basil (*Ocimum basilicum*) aqueous extract is mediated through inhibition of α-glucosidase and α-amylase activities: an in vitro study. Toxicol. Ind. Health 28, 42–50.

Eloff, J.N., 1998. Which extractant should be used for the screening and isolation of antimicrobial components from plants? J. Ethnopharmacol. 60, 1–8.

Gavanji, S., Mohabatkar, H., Baghshahi, H., Zarrabi, A., 2014. Bioinformatics prediction of interaction silver nanoparticles on the disulfide bonds of HIV-1 Gp120 protein. Int. J. Sci. Res. Knowl. 2, 67–74.

Gengan, R.M., Anand, K., Phulukdaree, A., Chuturgoon, A., 2013. A549 lung cell line activity of biosynthesized silver nanoparticles using *Albizia adianthifolia* leaf. Colloids Surf. B 105, 87–91.

German Homoeopathic Pharmacopoeia, 2005. German homoeopathic pharmacopoeia: GHP. Medpharm Scientific Publ, Stuttgart.

Govind, P., Madhuri, S., 2010. Pharmacological Activities of *Ocimum sanctum* (Tulsi): a Review. Int. J. Pharm. Sci. Rev. Res. 5, 61–66.

Guariguata, L., Whiting, D.R., Hambleton, I., Beagley, J., Linnenkamp, U., Shaw, J.E., 2014. Global estimates of diabetes prevalence for 2013 and projections for 2035. Diabetes Res. Clin. Pract. 103, 137–149.

Guo, D., Zhu, L., Huang, Z., Zhou, H., Ge, Y., Ma, W., Wu, J., Zhang, X., Zhou, X., Zhang, Y., Zhao, Y., Gu, N., 2013. Anti-leukemia activity of PVP-coated silver nanoparticles via generation of reactive oxygen species and release of silver ions. Biomaterials 34, 7884–7894.

Hall, V., Thomsen, R.W., Henriksen, O., Lohse, N., 2011. Diabetes in Sub Saharan Africa 1999–2011: epidemiology and public health implications. A systematic review. B.M.C. Public Health 11, 564.

Hannan, J.M., Marenah, L., Ali, L., Rokeya, B., Flatt, P.R., Abdel-Wahab, Y.H., 2006. *Ocimum sanctum* leaf extracts stimulate insulin secretion from perfused pancreas, isolated islets and clonal pancreatic beta-cells. J. Endocrinol. 189, 127–136.

Hannan, J.M.A., Ojo, O.O., Ali, L., Rokeya, B., Khaleque, J., Akhter, M., Flatt, P.R., Abdel-Wahab, Y.H.A., 2015. Actions underlying antidiabetic effects of *Ocimum sanctum* leaf extracts in animal models of type 1 and type 2 diabetes. Eur. J. Med. Plants 5, 1–12.

Huang, J., Li, Q., Sun, D., Lu, Y., Su, Y., Yang, X., Wang, H., Wang, Y., Shao, W., Ning, H., Hing, J., Chen, C., 2007. Biosynthesis of silver and gold nanoparticles by novel sundried *Cinna-mommum camphora* leaf. Nanotechnology 18, 104.

Jaiganesh, K.P., Baskar, N., Ramasamy, N., Arunachalam, G., 2012. Phytochemical and antimicrobial screening of *Ocimum basilicum*. Linn. J. Sci. Res. Pharm. 1, 102–106.

Joshi, B., Sah, G.P., Basnet, B.B., Bhatt, M.R., Sharma, D., Subedi, K., Pandey, J., Malla, R., 2011. Phytochemical extraction and antimicrobial properties of different medicinal plants: *Ocimum sanctum* (Tulsi), *Eugenia caryophyllata* (Clove), *Achyranthes bidentata* (Datiwan) and *Azadirachta indica* (Neem). J. Microbiol. Antimicrob. 3, 1–7.

Karthick, V., Kumar, V.G., Dhas, T.S., Singaravelu, G., Sadiq, A.M., Govindaraju, K., 2014. Effect of biologically synthesized gold nanoparticles on alloxan-induced diabetic rats-an in vivo approach. Colloids Surf. B 122, 505–511.

Kaya, I., Yiğit, N., Benli, M., 2009. Antimicrobial activity of various extracts of *Ocimum basilicum* L. and observation of the inhibition effect on bacterial cells by use of scanning electron microscopy. Afr. J. Tradit. Complement. Altern. Med. 5, 363–369.

Khogare, D.T., Lokhande, S.M., 2011. Effect of Tulasi (*Ocimum sanctum)* on diabetes mellitus. Indian Sreams Res. J. 1, 189–191.

Kim, M.J., Lee, S.B., Lee, H.S., Lee, S.Y., Baek, J.S., Kim, D., Moon, T.W., Robyt, J.F., Park, K.H., 1999. Comparative study of the inhibition of α-glucosidase, α-amylase, and cyclomaltodextrin glucanosyltransferase by acarbose, isoacarbose, and acarviosine-glucose. Arch. Biochem. Biophys. 371, 277–283.

Kotakadi, V.S., Gaddam, S.A., Rao, Y.S., Prasad, T.N.V.K.V., Reddy, A.V., Sai Gopal, D.V.R., 2014. Biofabrication of silver nanoparticles using *Andrographis paniculata*. Eur. J. Med. Chem. 73, 135–140.

Kothari, S.K., Bhattacharya, A.K., Ramesh, S., 2004. Essential oil yield and quality of methyl eugenol rich *Ocimum tenuiflorum* L.f. (Syn. *O. sanctum* L.) grown in south India as influenced by method of harvest. J. Chromatogr. A 1054, 67–72.

Krishnamoorthy, P., Jayalakshmi, T., 2012. Preparation, characterization and synthesis of silver nanoparticles by using *phyllanthus-niruri* for the antimicrobial activity and cytotoxic effects. J. Chem. Pharm. Res. 4, 4783–4794.

Kumari, M.M., Jacob, J., Philip, D., 2015. Green synthesis and applications of Au–Ag bimetallic nanoparticles. Spectrochim. Acta Mol. Biomol. Spectrosc. 137, 185–192.

Lee, S.J., Umano, K., Shibamoto, T., Lee, K.G., 2005. Identification of volatile components in basil (*Ocimum basilicum* L.) and thyme leaves (*Thymus vulgaris* L.) and their antioxidant properties. Food Chem. 91, 131–137.

Lokina, S., Stephen, A., Kaviyarasan, V., Arulvasu, C., Narayanan, V., 2014. Cytotoxicity and antimicrobial activities of green synthesized silver nanoparticles. Eur. J. Med. Chem. 76, 256–263.

Losasso, C., Belluco, S., Cibin, V., Zavagnin, P., Mičetić, I., Gallocchio, F., Zanella, M., Bregoli, L., Biancotto, G., Ricci, I., 2014. Antibacterial activity of silver nanoparticles: sensitivity of different *Salmonella* serovars. Front Microbiol. 5, 1–9.

Mccue, P.P., Shetty, K., 2004. Inhibitory effects of rosmarinic acid extracts on porcine pancreatic amylase in vitro. Asia Pac. J. Clin. Nutr. 13, 101–106.

Mo, R., Jiang, T., Di, J., Tai, W., Gu, Z., 2014. Emerging micro- and nanotechnology based synthetic approaches for insulin delivery. Chem. Soc. Rev. 43, 3595–3629.

Mogale, M.A., Lebelo, S.L., Thovhogi, N., De Freitas, A.N., Shai, L.J., 2011. Alpha-Amylase and alpha-glucosidase inhibitory effects of *Sclerocarya birrea* [(A. Rich.) Hochst.] subspecies caffra (Sond) Kokwaro (Anacardiaceae) stem-bark extracts. Afr. J. Biotech. 10, 15033–15039.

Morones, J.R., Elechiguerra, J.L., Camacho, A., Holt, K., Kouri, J.B., Yacaman, M.J., 2005. The bactericidal effect of silver nanoparticles. Nanotechnology 16, 2346–2353.

Mubarak, A.D., Thajuddin, N., Jeganathan, K., Gunasekaran, M., 2011. Plant extract mediated synthesis of silver and gold nanoparticles and its antibacterial activity against clinically isolated pathogens. Colloids Surf. B 85, 360–365.

Mukherjee, P., Maiti, K., Mukherjee, K., Houghton, P., 2006. Leads from Indian medicinal plants with hypoglycemic potentials. J. Ethnopharmacol. 106, 1–28.

Nguyen, T.H., Um, B.H., Kim, S.M., 2011. Two unsaturated fatty acids with potent α-glucosidase inhibitory activity purified from the

body wall of sea cucumber (*Stichopus japonicus*). J. Food Sci. 76, 208–214.

Panneerselvam, C., Murugan, K., Amerasan, D., 2015. Biosynthesis of silver nanoparticles using plant extract and its anti-plasmodial property. Adv. Mater. Res. 1086, 11–30, Trans. Tech. Publ..

Patel, D., Kumar, R., Laloo, D., Hemalatha, S., 2012. Diabetes mellitus: an overview on its pharmacological aspects and reported medicinal plants having antidiabetic activity. Asian Pac. J. Trop. Biomed. 2, 411–420.

Prabhu, D., Arulvasu, C., Babu, G., Manikandan, R., Srinivasan, P., 2013. Biologically synthesized green silver nanoparticles from leaf extract of *Vitex negundo* L. induce growth-inhibitory effect on human colon cancer cell line HCT15. Process Biochem. 48, 317–324.

Raman, S., Kandula, M.P., Jacob, J.A., Soundararajan, K., Ramar, T., Palani, G., Muthukalingan, K., Shanmugam, A., 2012. Cytotoxic effect of Green synthesized silver nanoparticles using *Melia azedarach* against in vitro HeLa cell lines and lymphoma mice model. Process Biochem. 47, 273–279.

Ramteke, C., Chakrabarti, T., Sarangi, B.K., Pandey, R.A., 2013. Synthesis of silver nanoparticles from the aqueous extract of leaves of *Ocimum sanctum* for enhanced antibacterial activity. J. Chem. 2013, 1–7.

Rao, Y.S., Kotakadi, V.S., Prasad, T.N.V.K.V., Reddy, A.V., Gopal, D.V.R.S., 2013. Green synthesis and spectral characterization of silver nanoparticles from Lakshmi tulasi (*Ocimum sanctum*) leaf extract. Spectrochim. Acta Mol. Biomol. Spectrosc. 103, 156–159.

Ratner, R.E., 2001. Glycemic control in the prevention of diabetic complications. Clin. Cornerstone 4, 24–37.

Reid, M.J.A., Tsima, B.M., Kirk, B., 2012. HIV and diabetes in Africa. Afr. J. Diabetes Med. 20, 28–32.

Rout, Y., Behera, S., Ojha, A.K., Nayak, P.L., 2012. Green synthesis of silver nanoparticles using *Ocimum sanctum* (Tulashi) and study of their antibacterial and antifungal activities. J. Microbiol. Antimicrob. 4, 103–109.

Saha, S., Dhar, T.N., Sengupta, C., Ghosh, P., 2013. Biological activities of essential oils and methanol extracts of five *Ocimum* species against pathogenic bacteria. Czech J. Food Sci. 31, 194–202.

Sahoo, S.K., Parveen, S., Panda, J.J., 2007. The present and future of nanotechnology in human health care. Nanomedicine 3, 20–31.

Shankar, E.M., Mohan, V., Premalatha, G., Srinivasan, R.S., Usha, A.R., 2005. Bacterial etiology of diabetic foot infections in South India. Eur. J. Intern. Med. 16, 567–570.

Singhal, G., Bhavesh, R., Kasariya, K., Sharma, A.R., Singh, R.P., 2011. Biosynthesis of silver nanoparticles using *Ocimum sanctum* (Tulsi) leaf extract and screening its antimicrobial activity. J. Nanopart. Res. 13, 2981–2988.

Sivaranjani, K., Meenakshisundaram, M., 2013. Biological synthesis of silver nanoparticles using *Ocimum basilicum* leaf extract and their antimicrobial activity. Int. Res. J. Pharm. 4, 225–229.

Sondi, I., Salopek-Sondi, B., 2004. Silver nanoparticles as antimicrobial agent: a case study on *E. coli* as a model for Gram-negative bacteria. J. Colloid Interface Sci. 275, 177–182.

Song, J.Y., Kim, B.S., 2009. Rapid biological synthesis of silver nanoparticles using plant leaf extracts. Bioprocess Biosyst. Eng. 32, 79–84.

Subramanian, R., Asmawi, M.Z., Sadikun, A., 2008. In vitro α-glucosidase and α-amylase enzyme inhibitory effects of *Andrographis paniculata* extract and *andrographolide*. Acta Biochim. Pol. 55, 391–398.

Sudha, P., Zinjarde, S., Bhargava, S., Kumar, A., 2011. Potent alpha-amylase inhibitory activity of Indian Ayurvedic medicinal plants. B.M.C. Complement Altern Med. 11 (5).

Swarnalatha, L., Rachela, C., Ranjanb, S., Baradwaj, P., 2012. Evaluation of in vitro antidiabetic activity of *Sphaeranthus Amaranthoides* silver nanoparticles. J. Nanomater. Biol. 2, 25–29.

Tudhope, L., 2008. The diabetic foot: protocols and current therapies. Wound Healing South Afr. 1, 37–39.

Usman, L.A., Ismaeel, R.O., Zubair, M.F., Saliu, B.K., Olawore, N.O., Elelu, N., 2013. Comparative studies of constituents and antibacterial activities of leaf and fruit essential oils of *Ocimium basilicum* grown in north central Nigeria. Int. J. Chem. Biol. Sci. 3, 47–52.

Venkatachalam, M., Govindaraju, K., Sadiq Mohamed, A., Tamilselvan, S., Ganesh Kumar, V., Singaravelu, G., 2013. Functionalization of gold nanoparticles as antidiabetic nanomaterial. Spectrochim. Acta A Mol. Biomol. Spectrosc. 116, 331–338.

Woldu, M.A., Lenjisa, J.L., 2014. Nanoparticles and the new era in diabetes management. Int J. Basic Clin. Pharmacol. 3, 277–284.

Please cite this article in press as: Malapermal, V. et al., Enhancing antidiabetic and antimicrobial performance of *Ocimum basilicum*, and *Ocimum sanctum* (L.) using silver nanoparticles. Saudi Journal of Biological Sciences (2015), http://dx.doi.org/10.1016/j.sjbs.2015.06.026